Current Biology 21, 391–398, March 8, 2011 ©2011 Elsevier Ltd All rights reserved DOI 10.1016/j.cub.2010.12.039

Report

Direct Binding of Cenp-C to the Mis12 Complex Joins the Inner and Outer Kinetochore

Emanuela Screpanti,[1,6] Anna De Antoni,[1,6] Gregory M. Alushin,[2] Arsen Petrovic,[1] Tiziana Melis,[1] Eva Nogales,[3,4] and Andrea Musacchio[1,5,*]

[1]Department of Experimental Oncology, European Institute of Oncology, Via Adamello 16, 20139 Milan, Italy
[2]Biophysics Graduate Group
[3]Howard Hughes Medical Institute, Department of Molecular and Cell Biology
University of California, Berkeley, Berkeley, CA 94720, USA
[4]Life Sciences Division, Lawrence Berkeley National Laboratory, Berkeley, CA 94720, USA
[5]Max Planck Institute of Molecular Physiology, 44227 Dortmund, Germany

Summary

Kinetochores are proteinaceous scaffolds implicated in the formation of load-bearing attachments of chromosomes to microtubules during mitosis. Kinetochores contain distinct chromatin- and microtubule-binding interfaces, generally defined as the inner and outer kinetochore, respectively (reviewed in [1]). The constitutive centromere-associated network (CCAN) and the Knl1-Mis12-Ndc80 complexes (KMN) network are the main multisubunit protein assemblies in the inner and outer kinetochore, respectively. The point of contact between the CCAN and the KMN network is unknown. Cenp-C is a conserved CCAN component whose central and C-terminal regions have been implicated in chromatin binding and dimerization [2–10]. Here, we show that a conserved motif in the N-terminal region of Cenp-C binds directly and with high affinity to the Mis12 complex. Expression in HeLa cells of the isolated N-terminal motif of Cenp-C prevents outer kinetochore assembly, causing chromosome missegregation. The KMN network is also responsible for kinetochore recruitment of the components of the spindle assembly checkpoint, and we observe checkpoint impairment in cells expressing the Cenp-C N-terminal segment. Our studies unveil a crucial and likely universal link between the inner and outer kinetochore.

Results and Discussion

The KMN network is a supramolecular assembly of the four-subunit Mis12 complex (abbreviated as Mis12C and containing Dsn1, Nnf1, Nsl1, and Mis12), the four-subunit Ndc80 complex (Ndc80C, containing Ndc80, Nuf2, Spc24, and Spc25), and the two-subunit Knl1 complex (Knl1C, containing Knl1 and Zwint). The inner core of the kinetochore is built on specialized chromatin containing the histone H3 variant Cenp-A as well as neighboring H3-containing nucleosomes (reviewed in [1]). A group of proteins, including Cenp-C, Cenp-H, Cenp-I, Cenp-K through Cenp-U, Cenp-W, and Cenp-X, comprises the constitutive centromere-associated network (CCAN, also known as NAC/CAD) and is closely associated with centromeric chromatin (reviewed in [1]). Within the CCAN, at least two subunits, Cenp-N and Cenp-C, contact Cenp-A directly [3, 5, 11].

Among the first kinetochore subunits to be cloned, Cenp-C (whose predicted domains are shown in Figure 1A) is enriched in affinity purifications of tagged subunits of the KMN network and is required for kinetochore recruitment of a subset of outer kinetochore proteins in different species [12–23]. Thus, Cenp-C might provide an attachment site for the recruitment of outer kinetochore components and their associated partners, including the components of the spindle assembly checkpoint. Here, we set out to formally test this hypothesis and describe an interaction responsible for these properties of Cenp-C.

The N-Terminal Region of Cenp-C Binds Directly to the Mis12 Complex

A Cenp-C deletion construct retaining only the C-terminal half of Cenp-C localizes normally to kinetochores but fails to recruit outer kinetochore components [18]. Thus, we initially tested whether a recombinant segment of Cenp-C encompassing residues 1–400 (Cenp-C$^{1–400}$) bound directly to recombinant KMN constituents reconstituted as recently described [24, 25]. When analyzed by size-exclusion chromatography (SEC, which separates based on size and shape), stoichiometric combinations of Cenp-C$^{1–400}$ and Ndc80C^{Bonsai} (an engineered Ndc80C retaining microtubule-binding and kinetochore-binding domains [24]) did not interact (see Figure S1A available online). Conversely, Cenp-C$^{1–400}$ interacted tightly with an engineered version of Mis12C in what appeared to be a 1:1 complex (Figure 1B). The Mis12C utilized in these experiments, Mis12C$^{Nsl1(1–227)}$, bears a 50-residue deletion in the C-terminal tail of the Nsl1 subunit that prevents the interaction of Nsl1 with Knl1 [25]. Additional deletion mutants of Mis12C, including Mis12C$^{Nsl1(1–258)}$, Mis12C^{Micro}, and Mis12C^{Mini} (the latter two bear additional deletions in the Nsl1 and Dsn1 subunit; see Supplemental Experimental Procedures), also interacted with Cenp-C$^{1–400}$ (Figure S1B and data not shown). Cenp-C$^{1–400}$ also interacted with the Mis12C-Knl1$^{2106–2316}$ complex, a complex of full-length Mis12C and the C-terminal region of Knl1 [25] (Figure 1C). Although Cenp-C was unable to bind Ndc80C^{Bonsai} or full length Ndc80C, a ternary complex was formed when Mis12C was also present (Figure 1D; Figures S1C and S1D). Overall, these results indicate that Cenp-C binds directly to Mis12C and that the interaction is compatible with additional interactions of Mis12C with Ndc80C and Knl1. The Cenp-C-Mis12C interaction appears stoichiometric, in agreement with a recent analysis of kinetochore subunit copy number [26].

Structural Analysis of KMN-Cenp-C Subcomplexes

When imaged by negative-stain electron microscopy, the human Ndc80C appears as a 60 nm flexible rod (Figure 2A). When in complex, Ndc80C and Mis12C add their lengths in series and appear as an ~80 nm whip, with a thicker "handle" corresponding to Mis12C (Figure 2B). This feature is emphasized in the complex of Ndc80C and Mis12C with Cenp-C$^{1–400}$ (Figure 2C). Images of the Mis12C and Mis12C-Cenp-C$^{1–400}$

*Correspondence: andrea.musacchio@ifom-ieo-campus.it
[6]These authors contributed equally to this work

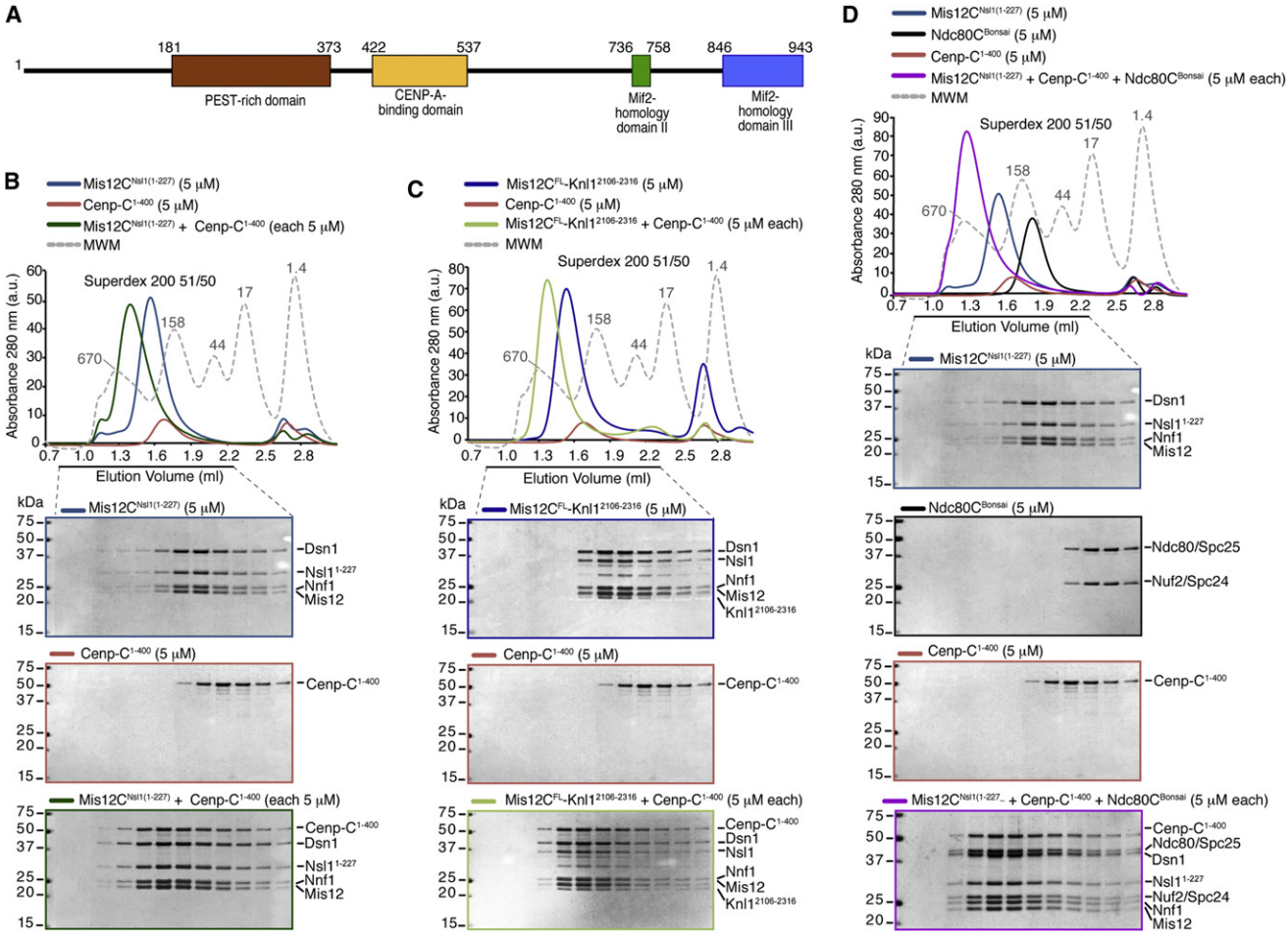

Figure 1. Cenp-C$^{1–400}$ Binds Mis12C

(A) Schematic depiction of the domain organization of human Cenp-C.

(B) Size-exclusion chromatography elution profiles and SDS-PAGE analysis of recombinant Mis12C$^{Nsl1(1–227)}$ (uppermost gel), recombinant Cenp-C$^{1–400}$ (middle), and their stoichiometric combination (lower). Complex formation is indicated by a shift in the elution profile of Cenp-C$^{1–400}$ and Mis12C$^{Nsl1(1–227)}$ and their appearance, in stoichiometric amounts, in early elution volumes.

(C) As in (B), but with Mis12C^{FL}-Knl1$^{2106–2316}$ instead of Mis12C$^{Nsl1(1–227)}$. The middle gel is the same as in (B).

(D) Incorporation of the Ndc80^{Bonsai} complex in the Cenp-C$^{1–400}$-Mis12C$^{Nsl1(1–227)}$ complex. The uppermost gel and the lower middle gel are the same as in (B). For more details, see Figure S1.

complexes in the absence of Ndc80C (Figures 2D and 2E) were used for 2D single-particle analysis (Figures 2F and 2G; Figure S2). Class averages of the Mis12C-Cenp-C$^{1–400}$ complex appear as a straight rod, generally with a globular domain visible at one end. In the absence of Cenp-C$^{1–400}$, the averages are far more heterogeneous, showing both straight and bent conformations, as well as variability in the presence or absence of a visible globular head domain. When the two data sets were mixed, our classification procedure robustly sorted them into classes that recaptured these essential features (Figure S2).

To investigate the complexes' flexibility, we constructed a simplified three-point model of each class average (Figure 2H), with points placed at the center of the globular head, the hinge point, and the tip of the tail. We then measured the bending angle, θ, for each modeled class average. When weighted by the particle distribution across the classes, histograms of the bending-angle distribution present in each sample population demonstrate far greater rigidity of the complex in the presence of Cenp-C$^{1–400}$ (Figure 2H). Nevertheless, the Mis12 complex can access straight conformations in the absence of Cenp-C$^{1–400}$, albeit infrequently relative to bent ones.

We applied chemical crosslinking methods to identify potential sites of contact between Cenp-C and the Mis12 complex, but the data, as a result of technical limitations, were not conclusive (data not shown). The electron microscopy analysis also did not provide a firm localization of Cenp-C, because there is no strong additional density present in the Mis12C-Cenp-C$^{1–400}$ complex averages that does not appear in the averages of the Mis12C alone (Figure S2), despite the differences in the conformational landscapes of the two populations. This suggests that the majority of Cenp-C$^{1–400}$ is flexible relative to Mis12C, in agreement with the small portion of Cenp-C$^{1–400}$ that is sufficient for Mis12C binding (see below).

Mis12C Binds a 20-Residue Motif in the N-Terminal Region of Cenp-C

Next, we sought to dissect the Cenp-C region mediating the interaction with Mis12C. We created progressively shorter

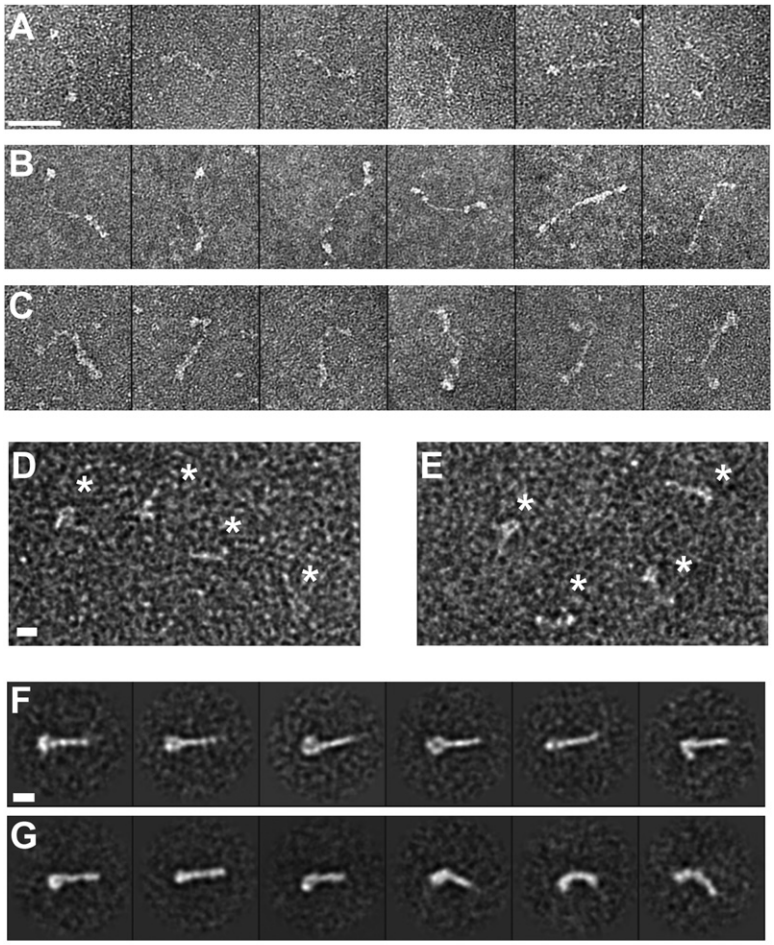

Figure 2. Electron Microscopy Analysis of the Cenp-C-Mis12C Complex

(A) Representative single particles of human Ndc80C (full length). Scale bar represents 50 nm.

(B) Representative single particles of Ndc80C-Mis12C$^{Nsl1(1–258)}$.

(C) Representative single particles of Ndc80C-Mis12C$^{Nsl1(1–258)}$-Cenp-C$^{1–400}$.

(D) Representative field of single particles of the Mis12C$^{Nsl1(1–258)}$-Cenp-C$^{1–400}$ complex. Particles are indicated by asterisks. Scale bar represents 10 nm.

(E) Representative field of particles of Mis12C$^{Nsl1(1–258)}$. Additional analyses of this complex have been recently published [25, 39, 40].

(F) Selected reference-free class averages of the Mis12C$^{Nsl1(1–258)}$-Cenp-C$^{1–400}$ complex. The complex appears as a linear rod, generally with a prominent bump at one end. Scale bar represents 10 nm.

(G) Selected reference-free class averages of Mis12C$^{Nsl1(1–258)}$ alone. The complex adopts varying degrees of bending, and the globular lobe is often absent or diminished in size.

(H) Bending-angle analysis of the Mis12 complex in the presence and absence of Cenp-C$^{1–400}$. The complex is substantially rigidified upon Cenp-C binding.

For more details, see Figure S2.

GST fusions of the N-terminal region of Cenp-C and tested their ability to bind Mis12C (data not shown). GST-Cenp-C$^{1–71}$ coeluted with Mis12C from a size-exclusion column (Figure 3A), and the same was true for Cenp-C$^{1–71}$ after removal of the GST moiety (Figure S3A).

Cenp-C$^{1–71}$ contains two short conserved motifs and is predicted to fold as three consecutive helices (Figure 3B). We tested the effects of several single alanine point mutations in conserved residues. Substitutions K10A and Y13A in predicted helix αA reduced the interaction between Cenp-C$^{1–71}$ and the Mis12 complex (Figures 3C and 3D). On the other hand, introduction of alanine mutations in additional residues, including R19A and F42A in predicted helix αB, did not affect Mis12C binding (Figures S3B and S3C). Essentially identical results were obtained when the chromatography experiments were performed with the isolated Cenp-C$^{1–71}$ segment and related mutants after cleavage of the GST moiety (data not shown). Overall, these results indicate that the Mis12C-binding site of Cenp-C maps to a conserved (predicted) helix in the N-terminal region of Cenp-C. In agreement with this idea, further C-terminal deletions of Cenp-C, including Cenp-C$^{1–46}$ and Cenp-C$^{1–21}$, also coeluted with Mis12C in SEC runs (Figures S3D and S3E).

Effects from Impairing the Cenp-C-Mis12 Interaction in Cells

To gain an indicative estimate of the binding affinity of the interaction, we carried out a fluorescence polarization assay on the interaction of Mis12C with a synthetic fluorescein-conjugated peptide corresponding to Cenp-C$^{1–21}$. The dissociation constant (K_D) of the interaction was 629 ± 38 nM (Figure 4A). Thus, Cenp-C$^{1–71}$ binds directly to Mis12C in vitro with high affinity. Based on these findings, we reasoned that overexpression of the N-terminal segment of Cenp-C in cells might prevent Mis12C recruitment to kinetochores through competition with endogenous Cenp-C. GFP-Cenp-C (full length) stained kinetochores when expressed in HeLa cells after transient transfection, indicating that GFP fusions at the N terminus of Cenp-C do not interfere with Cenp-C kinetochore recruitment (Figure S4). GFP-Cenp-C$^{1–71}$, on the other hand, was not recruited to kinetochores and showed diffuse cytosolic staining in mitotic HeLa cells (Figure 4B). This is in agreement with previous studies showing that the N-terminal region of Cenp-C is dispensable for kinetochore targeting [3, 10, 18].

In agreement with our in vitro analysis (Figure 1; Figure 2; Figure 3), immunoprecipitates revealed Mis12, Ndc80, Knl1, and the Knl1-associated subunit Zwint as binding partners of GFP-Cenp-C$^{1–71}$ (Figure 4C; Figure S5F) Because GFP-Cenp-C$^{1–71}$ does not localize to kinetochores, its overexpression is expected to prevent kinetochore localization of its binding partners during mitosis. Indeed, kinetochore localization of Mis12, Knl1, and Zwint was abrogated upon expression of GFP-Cenp-C$^{1–71}$ (Figure 4B; Figure S5). Kinetochore

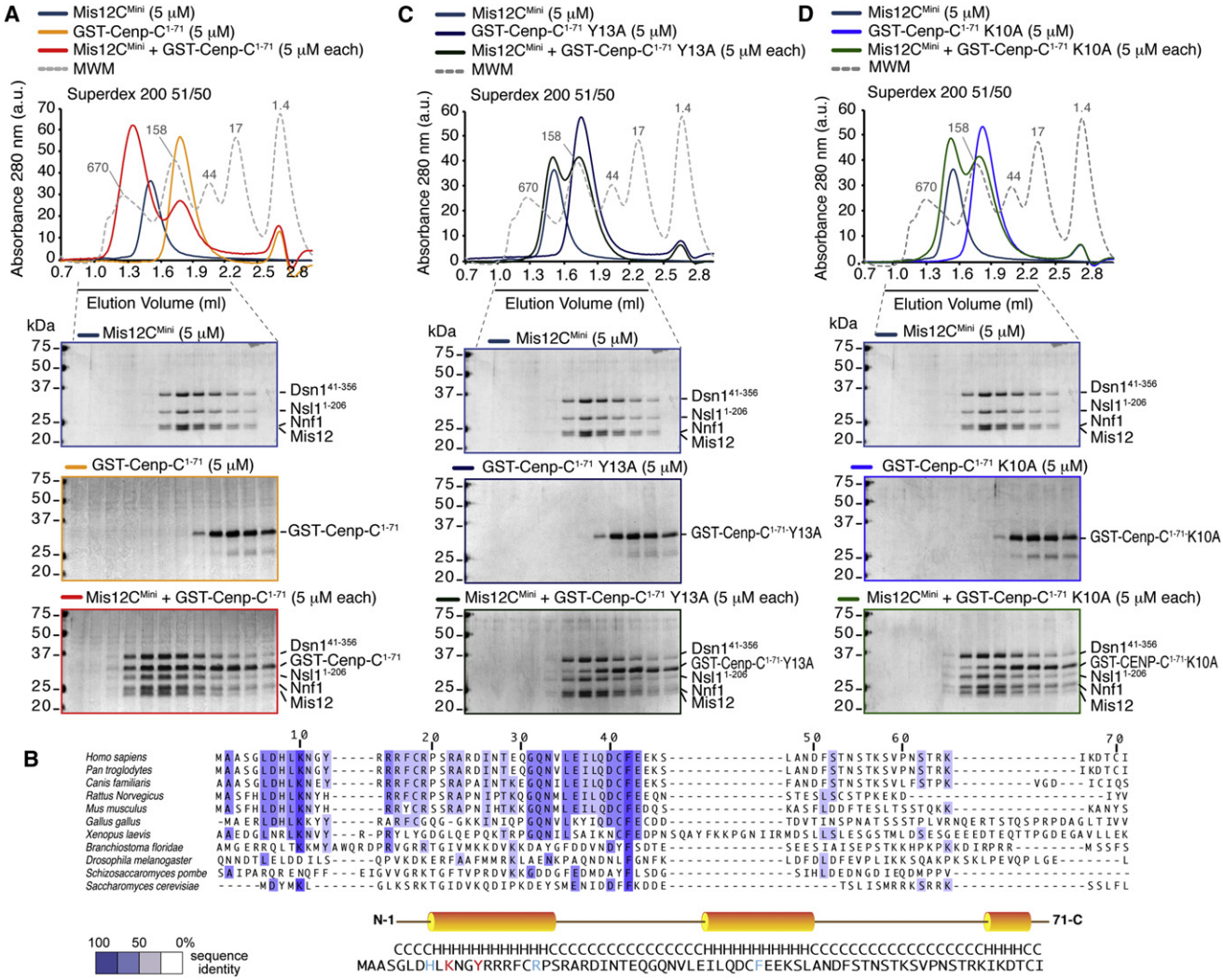

Figure 3. Wild-Type but Not Mutant Cenp-C$^{1–71}$ Binds Mis12C

(A) Size-exclusion chromatography elution profiles and SDS-PAGE analysis of recombinant Mis12C^{Mini} (uppermost gel), recombinant GST-Cenp-C$^{1–71}$ (middle), and their stoichiometric combination (lower). Complex formation is indicated by a shift in the elution profile of GST-Cenp-C$^{1–71}$ and Mis12C^{Mini} and their appearance, in stoichiometric amounts, in early elution volumes.

(B) Multiple sequence alignment of the N-terminal region of Cenp-C from the indicated species. The coloring scheme indicates the degree of conservation (see key at lower left). Below, the position of three predicted helices is shown on the sequence of human Cenp-C.

(C) As in (A), but with a GST-Cenp-C$^{1–71}$-Y13A mutant. The upper gel is the same as in (A). No shift in elution volume is observed, indicating that binding is impaired.

(D) As in (A), but with a GST-Cenp-C$^{1–71}$-K10A mutant. The upper gel is the same as in (A). No shift in elution volume is observed with this mutant either. For more details, see Figure S3.

localization of Ndc80 was significantly reduced, although small residual amounts of this protein remained visible (Figure 4D). On the other hand, mislocalization of outer kinetochore subunits was not observed upon expression of the GFP-Cenp-C$^{1–71}$-K10A/Y13A double mutant (Figures 4B and 4D; Figure S5). These results demonstrate that the overexpression of GFP-Cenp-C$^{1–71}$ prevents the recruitment of the KMN network to the outer kinetochore.

Impaired Chromosome Segregation in Cells Expressing Cenp-C$^{1–71}$

Next, we monitored the progression of cells expressing Cenp-C$^{1–71}$ or Cenp-C$^{1–71}$-K10A/Y13A through mitosis. We performed time-lapse video microscopy on HeLa cells (stably expressing histone H2B-Cherry to mark chromosomes) transfected with GFP-Cenp-C$^{1–71}$ or GFP-Cenp-C$^{1–71}$-K10A/Y13A (Figures 5A and 5B). In 6 of 6 cells transfected with the GFP-Cenp-C$^{1–71}$ construct, we observed a dramatic chromosome segregation phenotype. Chromosomes in these cells were unable to form a clear metaphase plate. All cells exited mitosis prematurely in the absence of a metaphase plate. None of these effects were observed in cells expressing the GFP-Cenp-C$^{1–71}$-K10A/Y13A construct, which instead divided normally (16 cells observed).

Cells expressing GFP-Cenp-C$^{1–71}$ appear to be unable to mount a strong checkpoint response, because they exit mitosis prematurely with many unattached or incorrectly attached chromosomes (Figures 5A and 5B). Mis12C has been shown to be important for direct or indirect kinetochore recruitment of several checkpoint components [19, 27]. Correspondingly,

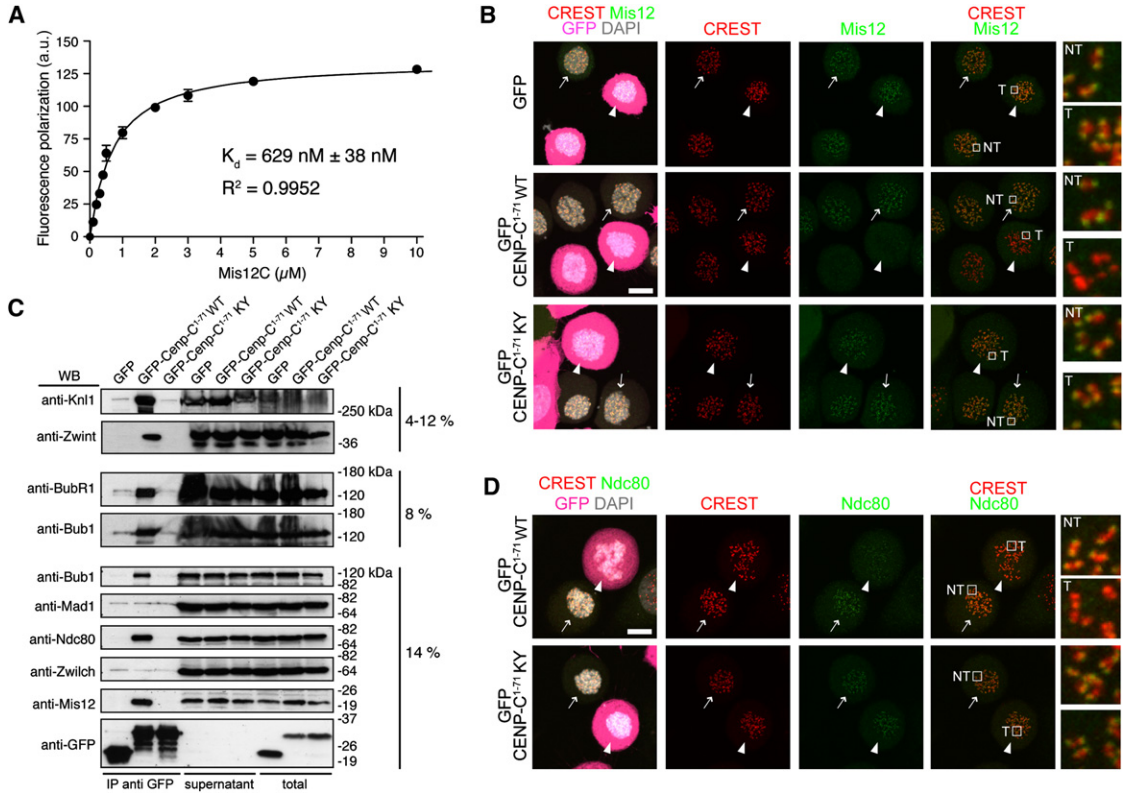

Figure 4. Cenp-C$^{1–71}$ Disrupts Outer Kinetochore Assembly

(A) Fluorescence anisotropy measurements of the binding affinity of Mis12^{Mini} for a synthetic fluorescein-conjugated peptide encompassing residues 1–21 of Cenp-C. Error bars represent standard deviation.

(B) Direct fluorescence (GFP and DAPI) or indirect immunofluorescence from the indicated species in HeLa cells. In (B) and (D), arrows indicate nontransfected GFP-negative cells whereas arrowheads indicate transfected GFP-positive cells. Localization of Mis12 in GFP-transfected cells is normal. Mis12 is displaced from kinetochores in cells expressing the wild-type sequence of GFP-Cenp-C$^{1–71}$. The construct localizes in the cytosol, but it is not enriched at kinetochores. Mis12 is normally localized in cells expressing the double point mutant GFP-Cenp-C$^{1–71}$-K10A/Y13A (abbreviated as KY). Scale bar represents 10 μm.

(C) Lysates from HeLa cells expressing the indicated GFP species were used for immunoprecipitations with an anti-GFP antibody. Several outer kinetochore proteins interact with wild-type GFP-Cenp-C$^{1–71}$ but not with its mutated form. Contents of immunoprecipitations from 1.5 mg of cell lysates, 45 μg of supernatants, and 45 μg of total cell lysates were loaded on gels.

(D) As in (B), but detecting Ndc80.

For more details, see Figures S4 and S5.

we found that besides KMN subunits, the GFP-Cenp-C$^{1–71}$ precipitates also contained Bub1 and BubR1 (Figure 4B). Indeed, both Bub1 and BubR1 were displaced from kinetochores in HeLa cells expressing GFP-Cenp-C$^{1–71}$ (Figure 5C; Figure S5B). Although Mad1 and Zwilch, two additional checkpoint components, were not identified in the GFP-Cenp-C$^{1–71}$ immunoprecipitates, they too were variably mislocalized upon expression of GFP-Cenp-C$^{1–71}$ (Figures S5C–S5E), in agreement with a previously established requirement for Mis12C in their kinetochore recruitment [19, 27]. Because Ndc80 is required for kinetochore localization of Zwilch and Mad1, we suspect that its residual kinetochore localization in cells expressing GFP-Cenp-C$^{1–71}$ is responsible for residual Mad1 and Zwilch recruitment (Figures S5C–S5E). These residual amounts of checkpoint proteins in turn might explain the residual checkpoint response observed in Figures 5A and 5B.

Conclusions

We report here that the N-terminal region of Cenp-C contains a crucial link between the inner and outer kinetochore (Figure 5D). The identification of Mis12C as a direct binding partner of Cenp-C is consistent with recent superresolution analyses of the kinetochore [28–30]. These have indicated that the N-terminal region of Cenp-C is positioned on a plane perpendicular to the interkinetochore axis, which also hosts Mis12C subunits.

The evolutionary conservation of the Mis12-binding motif suggests that its role may be universal. In certain organisms, such as *C. elegans* and *D. melanogaster*, no homologs of the CCAN subunits, with the exception of Cenp-C, have been identified thus far. In these organisms, the interaction between Cenp-C and Mis12C might provide the only linkage between the inner and outer kinetochore (Figure 5E), as strongly suggested by an accompanying paper in this issue of *Current Biology* reporting an analysis of the interaction of Cenp-C and Mis12 complex subunits in *D. melanogaster* [31].

In most other organisms, including humans, additional contacts between the CCAN and the KMN network likely exist. Kinetochore recruitment of Ndc80C in the absence of Knl1 is unaltered, and it is reduced but not eliminated upon depletion

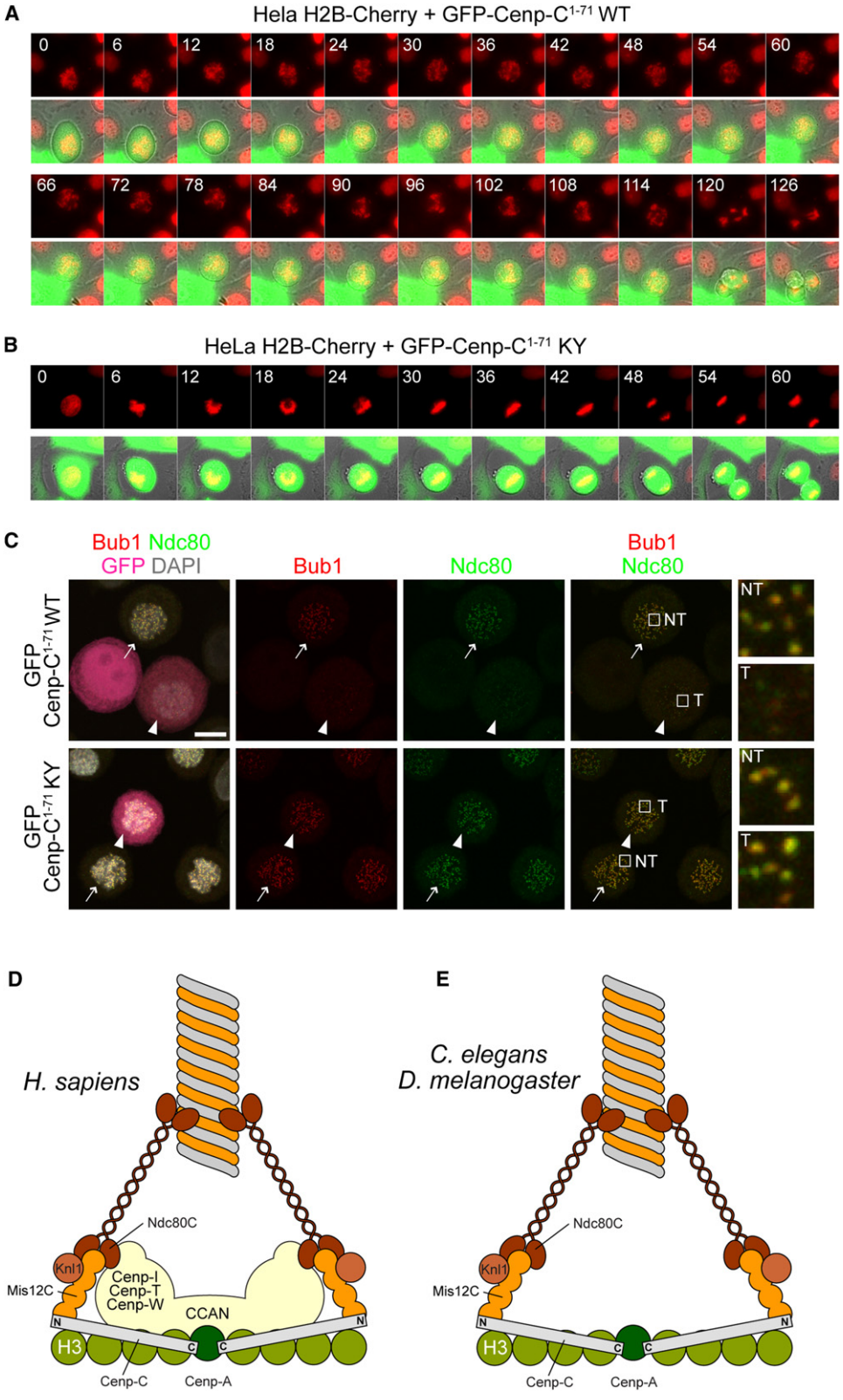

Figure 5. Cenp-C$^{1-71}$ Disrupts the Spindle Checkpoint

(A) HeLa cells coexpressing histone H2B-Cherry and wild-type GFP-Cenp-C$^{1-71}$ were filmed as they transited through mitosis. Cells attempted congression but failed to align and exited aberrantly, indicative of spindle checkpoint failure.

(B) HeLa cells coexpressing histone H2B-Cherry and mutant GFP-Cenp-C$^{1-71}$-K10A/Y13A divided normally.

(C) Direct fluorescence (GFP and DAPI) or indirect immunofluorescence from the indicated species in HeLa cells. Arrows indicate nontransfected GFP-negative cells whereas arrowheads indicate transfected GFP-positive cells. Localization of Bub1 and Ndc80 is severely impaired in cells expressing

of Mis12C subunits [19, 27, 32–34]. We confirmed these previous observations, because we consistently observed residual kinetochore levels of Ndc80 in cells expressing a dominant-negative construct of Cenp-C. These observations justify a two-hand model of outer kinetochore assembly [25, 33] in which Ndc80C is recruited via Mis12C as well as via another point of contact with the CCAN, probably involving proteins such as Cenp-I, Cenp-T, and Cenp-W [19, 35].

How does Cenp-C act as a linker between the inner and outer kinetochore? There are DNA-binding and dimerization domains in the central and C-terminal region of Cenp-C [2–10]. One such domain binds directly to a Cenp-A-containing specialized centromeric nucleosome [5] (Figure 1A). A crucial question for future studies is whether the interaction of Cenp-C with Mis12 occurs on the same specialized Cenp-A-containing centromeric nucleosome or rather on neighboring H3-containing nucleosomes. The reported association of Cenp-C and additional centromeric proteins with H3-containing nucleosomes supports the latter hypothesis [36]. In this scheme, Cenp-C might act as a ruler in the inner kinetochore plate (Figures 5D and 5E). We speculate that Cenp-C contributes to docking the outer kinetochore KMN network at the required distance from a "center" marked by one or more Cenp-A nucleosomes.

The significance of Cenp-C's rigidifying the Mis12 complex is unclear and is also an important subject for future study. Structural transitions in the Mis12 complex have been observed in superresolution studies in response to kinetochore-microtubule attachment state [30]. Our results suggest that interaction with inner kinetochore subunits also modulates the conformation of this complex. It is tempting to speculate that Cenp-C binding biases Mis12 toward a conformation suitable for interaction with other cellular factors specifically when it is localized to kinetochores.

Remarkably, the Aurora B-containing chromosome-passenger complex, which regulates crucial aspects of spindle checkpoint signaling and outer kinetochore function, also associates with H3-containing nucleosomes through a modification of the H3 N-terminal tail (reviewed in [37]). Aurora B localization is perturbed when Cenp-C is depleted or when the interaction of the Mis12 complex with HP1 (heterochromatin protein 1, a histone tail-binding protein) is affected [22, 38]. All of these clues point to the existence of a specialized structure in the inner kinetochore holding H3-containing and Cenp-A-containing nucleosomes in close proximity and possibly interacting through Cenp-C and other subunits.

Supplemental Information

Supplemental Information includes five figures and Supplemental Experimental Procedures and can be found with this article online at doi:10.1016/j.cub.2010.12.039.

Acknowledgments

We thank Sebastiano Pasqualato, Silvia Monzani, and Lucia Massimiliano for providing reagents and the members of the Musacchio laboratory for many helpful discussions. Work in the Musacchio laboratory is generously funded by the Association for International Cancer Research, Programmi Integrati di Oncologia Strategici 7/07, the FP7 European Research Council contract KINCON and the Integrated Project MitoSys (grant agreement number 241548), the Italian Association for Cancer Research (AIRC), the Cariplo Foundation, and the Human Frontier Science Program. Work in the Nogales laboratory is funded by the National Institute of General Medical Sciences. G.M.A. is partially funded by a National Institutes of Health training grant. E.S. is supported by a fellowship of the Italian Foundation for Cancer Research (FIRC). E.N. is a Howard Hughes Medical Institute Investigator.

Received: November 17, 2010
Revised: December 16, 2010
Accepted: December 17, 2010
Published online: February 24, 2011

References

1. Santaguida, S., and Musacchio, A. (2009). The life and miracles of kinetochores. EMBO J. *28*, 2511–2531.
2. Trazzi, S., Bernardoni, R., Diolaiti, D., Politi, V., Earnshaw, W.C., Perini, G., and Della Valle, G. (2002). In vivo functional dissection of human inner kinetochore protein CENP-C. J. Struct. Biol. *140*, 39–48.
3. Trazzi, S., Perini, G., Bernardoni, R., Zoli, M., Reese, J.C., Musacchio, A., and Della Valle, G. (2009). The C-terminal domain of CENP-C displays multiple and critical functions for mammalian centromere formation. PLoS ONE *4*, e5832.
4. Cohen, R.L., Espelin, C.W., De Wulf, P., Sorger, P.K., Harrison, S.C., and Simons, K.T. (2008). Structural and functional dissection of Mif2p, a conserved DNA-binding kinetochore protein. Mol. Biol. Cell *19*, 4480–4491.
5. Carroll, C.W., Milks, K.J., and Straight, A.F. (2010). Dual recognition of CENP-A nucleosomes is required for centromere assembly. J. Cell Biol. *189*, 1143–1155.
6. Song, K., Gronemeyer, B., Lu, W., Eugster, E., and Tomkiel, J.E. (2002). Mutational analysis of the central centromere targeting domain of human centromere protein C, (CENP-C). Exp. Cell Res. *275*, 81–91.
7. Meluh, P.B., and Koshland, D. (1997). Budding yeast centromere composition and assembly as revealed by in vivo cross-linking. Genes Dev. *11*, 3401–3412.
8. Sugimoto, K., Yata, H., Muro, Y., and Himeno, M. (1994). Human centromere protein C (CENP-C) is a DNA-binding protein which possesses a novel DNA-binding motif. J. Biochem. *116*, 877–881.
9. Yang, C.H., Tomkiel, J., Saitoh, H., Johnson, D.H., and Earnshaw, W.C. (1996). Identification of overlapping DNA-binding and centromere-targeting domains in the human kinetochore protein CENP-C. Mol. Cell. Biol. *16*, 3576–3586.
10. Lanini, L., and McKeon, F. (1995). Domains required for CENP-C assembly at the kinetochore. Mol. Biol. Cell *6*, 1049–1059.
11. Carroll, C.W., Silva, M.C., Godek, K.M., Jansen, L.E., and Straight, A.F. (2009). Centromere assembly requires the direct recognition of CENP-A nucleosomes by CENP-N. Nat. Cell Biol. *11*, 896–902.
12. Saitoh, H., Tomkiel, J., Cooke, C.A., Ratrie, H., 3rd, Maurer, M., Rothfield, N.F., and Earnshaw, W.C. (1992). CENP-C, an autoantigen in scleroderma, is a component of the human inner kinetochore plate. Cell *70*, 115–125.
13. Cheeseman, I.M., Niessen, S., Anderson, S., Hyndman, F., Yates, J.R., 3rd, Oegema, K., and Desai, A. (2004). A conserved protein network controls assembly of the outer kinetochore and its ability to sustain tension. Genes Dev. *18*, 2255–2268.
14. Westermann, S., Cheeseman, I.M., Anderson, S., Yates, J.R., 3rd, Drubin, D.G., and Barnes, G. (2003). Architecture of the budding yeast kinetochore reveals a conserved molecular core. J. Cell Biol. *163*, 215–222.

GFP-Cenp-C$^{1-71}$, whereas it is normal in cells expressing the double point mutant GFP-Cenp-C$^{1-71}$K10A/Y13A (abbreviated as KY). Scale bar represents 10 μm.

(D) Model for the interaction of the inner and outer kinetochore in mammalian cells. A "two-hand" model predicts that Ndc80 is recruited in part via Mis12C, but also through a pathway that depends on the constitutive centromere-associated network (CCAN). Only the globular C-terminal domain of Knl1 is shown.

(E) The CCAN is not present in *D. melanogaster* or *C. elegans*, suggesting that the interaction of Mis12C with Cenp-C is the only contact between the inner and outer kinetochore.

For more details, see Figure S5.

15. De Wulf, P., McAinsh, A.D., and Sorger, P.K. (2003). Hierarchical assembly of the budding yeast kinetochore from multiple subcomplexes. Genes Dev. *17*, 2902–2921.
16. Pinsky, B.A., Tatsutani, S.Y., Collins, K.A., and Biggins, S. (2003). An Mtw1 complex promotes kinetochore biorientation that is monitored by the Ipl1/Aurora protein kinase. Dev. Cell *5*, 735–745.
17. Desai, A., Rybina, S., Müller-Reichert, T., Shevchenko, A., Shevchenko, A., Hyman, A., and Oegema, K. (2003). KNL-1 directs assembly of the microtubule-binding interface of the kinetochore in C. elegans. Genes Dev. *17*, 2421–2435.
18. Milks, K.J., Moree, B., and Straight, A.F. (2009). Dissection of CENP-C-directed centromere and kinetochore assembly. Mol. Biol. Cell *20*, 4246–4255.
19. Liu, S.T., Rattner, J.B., Jablonski, S.A., and Yen, T.J. (2006). Mapping the assembly pathways that specify formation of the trilaminar kinetochore plates in human cells. J. Cell Biol. *175*, 41–53.
20. Kwon, M.S., Hori, T., Okada, M., and Fukagawa, T. (2007). CENP-C is involved in chromosome segregation, mitotic checkpoint function, and kinetochore assembly. Mol. Biol. Cell *18*, 2155–2168.
21. Przewloka, M.R., Zhang, W., Costa, P., Archambault, V., D'Avino, P.P., Lilley, K.S., Laue, E.D., McAinsh, A.D., and Glover, D.M. (2007). Molecular analysis of core kinetochore composition and assembly in Drosophila melanogaster. PLoS ONE *2*, e478.
22. Orr, B., and Sunkel, C.E. (2011). Drosophila CENP-C is essential for centromere identity. Chromosoma *120*, 83–96.
23. Tanaka, K., Chang, H.L., Kagami, A., and Watanabe, Y. (2009). CENP-C functions as a scaffold for effectors with essential kinetochore functions in mitosis and meiosis. Dev. Cell *17*, 334–343.
24. Ciferri, C., Pasqualato, S., Screpanti, E., Varetti, G., Santaguida, S., Dos Reis, G., Maiolica, A., Polka, J., De Luca, J.G., De Wulf, P., et al. (2008). Implications for kinetochore-microtubule attachment from the structure of an engineered Ndc80 complex. Cell *133*, 427–439.
25. Petrovic, A., Pasqualato, S., Dube, P., Krenn, V., Santaguida, S., Cittaro, D., Monzani, S., Massimiliano, L., Keller, J., Tarricone, A., et al. (2010). The MIS12 complex is a protein interaction hub for outer kinetochore assembly. J. Cell Biol. *190*, 835–852.
26. Johnston, K., Joglekar, A., Hori, T., Suzuki, A., Fukagawa, T., and Salmon, E.D. (2010). Vertebrate kinetochore protein architecture: Protein copy number. J. Cell Biol. *189*, 937–943.
27. McAinsh, A.D., Meraldi, P., Draviam, V.M., Toso, A., and Sorger, P.K. (2006). The human kinetochore proteins Nnf1R and Mcm21R are required for accurate chromosome segregation. EMBO J. *25*, 4033–4049.
28. Joglekar, A.P., Bloom, K., and Salmon, E.D. (2009). In vivo protein architecture of the eukaryotic kinetochore with nanometer scale accuracy. Curr. Biol. *19*, 694–699.
29. Schittenhelm, R.B., Heeger, S., Althoff, F., Walter, A., Heidmann, S., Mechtler, K., and Lehner, C.F. (2007). Spatial organization of a ubiquitous eukaryotic kinetochore protein network in Drosophila chromosomes. Chromosoma *116*, 385–402.
30. Wan, X., O'Quinn, R.P., Pierce, H.L., Joglekar, A.P., Gall, W.E., DeLuca, J.G., Carroll, C.W., Liu, S.T., Yen, T.J., McEwen, B.F., et al. (2009). Protein architecture of the human kinetochore microtubule attachment site. Cell *137*, 672–684.
31. Przewloka, M.R., Venkei, Z., Bolanos-Garcia, V.M., Debski, J., Dadlez, M., and Glover, D.M. (2011). CENP-C is a structural platform for kinetochore assembly. Curr. Biol. *20*, this issue, 399–405.
32. Kline, S.L., Cheeseman, I.M., Hori, T., Fukagawa, T., and Desai, A. (2006). The human Mis12 complex is required for kinetochore assembly and proper chromosome segregation. J. Cell Biol. *173*, 9–17.
33. Cheeseman, I.M., Hori, T., Fukagawa, T., and Desai, A. (2008). KNL1 and the CENP-H/I/K complex coordinately direct kinetochore assembly in vertebrates. Mol. Biol. Cell *19*, 587–594.
34. Kiyomitsu, T., Obuse, C., and Yanagida, M. (2007). Human Blinkin/AF15q14 is required for chromosome alignment and the mitotic checkpoint through direct interaction with Bub1 and BubR1. Dev. Cell *13*, 663–676.
35. Hori, T., Okada, M., Maenaka, K., and Fukagawa, T. (2008). CENP-O class proteins form a stable complex and are required for proper kinetochore function. Mol. Biol. Cell *19*, 843–854.
36. Hori, T., Amano, M., Suzuki, A., Backer, C.B., Welburn, J.P., Dong, Y., McEwen, B.F., Shang, W.H., Suzuki, E., Okawa, K., et al. (2008). CCAN makes multiple contacts with centromeric DNA to provide distinct pathways to the outer kinetochore. Cell *135*, 1039–1052.
37. Vader, G., and Lens, S.M. (2010). Chromosome segregation: Taking the passenger seat. Curr. Biol. *20*, R879–R881.
38. Kiyomitsu, T., Iwasaki, O., Obuse, C., and Yanagida, M. (2010). Inner centromere formation requires hMis14, a trident kinetochore protein that specifically recruits HP1 to human chromosomes. J. Cell Biol. *188*, 791–807.
39. Maskell, D.P., Hu, X.W., and Singleton, M.R. (2010). Molecular architecture and assembly of the yeast kinetochore MIND complex. J. Cell Biol. *190*, 823–834.
40. Hornung, P., Maier, M., Alushin, G.M., Lander, G.C., Nogales, E., and Westermann, S. (2011). Molecular architecture and connectivity of the budding yeast Mtw1 kinetochore complex. J. Mol. Biol. *405*, 548–559.